Korean J. Chem. Eng., **27**(1), 324-327 (2010)
DOI: 10.1007/s11814-009-0314-4

Dependence of approaching velocity on the force-distance curve in AFM analysis

Younghun Kim*,†, Young In Yang, Inhee Choi**, and Jongheop Yi****

*Department of Chemical Engineering, Kwangwoon University, Seoul 139-701, Korea
**School of Chemical & Biological Engineering, Seoul National University, Seoul 151-742, Korea
(*Received 22 May 2009 • accepted 24 June 2009*)

Abstract−The force-distance (F-D) curve in AFM analysis is a useful technique in the field of biophysics and surface science for measuring the physical/chemical properties of a substrate. Herein, the dependence of V_z on the F-D curve has been described via a theoretical investigation confirmed with measured data. The results show the attractive force was gradually reduced above a V_z of 5 μm/s by increasing the external repulsive force loaded onto the cantilever. To obtain a non-distorted F-D curve, one of two methods should be used: to analyze F-D curve under V_z of 1 μm/s or use of a short/stiff cantilever.

Key words: AFM, Image Disrotion, Force-distance Curve

INTODUCTION

Atomic force microscopy (AFM) has emerged as a useful tool for the microscopic reading the surface morphology [1], lithographic writing of the nanopattern onto a substrate [2], and spectroscopic measuring of the conductance between two electrodes [3]. Among these applications, force-distance (F-D) analysis is a fundamental tool in several fields of research, such as surface science, materials engineering, biochemistry and biology. In these fields, F-D curves are routinely used to determine several kinds of measurements, such as elasticity, adhesion energy, Hamaker constants, surface charge densities and degrees of hydrophobicity [4]. In a previous report, Evans and others used the biomembrane force probe to test the adhesive strengths of attachments between surface-bound P-selectin, and showed the loading rate is highly dependent upon the rupture force and unbinding force [5]. A classical molecular dynamics was also used to investigate the interfacial adhesion between polyester and carbon-based particles [6,7].

The most interesting regions of F-D curves are the non-contact regions, containing the jump-to-contact and jump-off-contact points, which provide information about the attractive and repulsive forces both before and after contact. In particular, the measured force at the jump-off-contact point relates to the contact adhesive stress, from which the adhesion energy can easily be obtained by integration of the triangular area (gray region of inset in Fig. 1) at this point [8].

When the F-D curves for the mica/NSC36C (L=130 μm and k= 0.60 N/m) system were measured using a different approaching velocity (V_z=0.1, 1, and 5 μm/s), as illustrated in Fig. 1, they revealed different jump-off-contact forces, resulting in a different adhesion energy in relation to the approaching velocity. As V_z decreased, the attraction energy gradually increased, and the F-D curve showed a more negative value. It should be noted that the approaching (or retracting) velocity had a big impact on the attraction force in the F-D curve measurement. This feature distorted the F-D curve between the tip and the substrate, making it difficult to obtain the exact adhesion energy from F-D curve. However, there is less information in the literature on the effect of the approaching/retracting velocity for measuring F-D curves. Therefore, the importance of the approaching/retracting velocity for measuring the F-D curve in AFM analysis was investigated.

EXPERIMENTAL SECTION

To obtain the F-D curve between the mica and the probe tip, a commercial AFM instrument (XE-100, Park System, Korea) was used. To minimize the intrinsic distortion of the apparatus, an independent *z*-scanner was used, which also eliminated the *x*-*z* cross coupling problem inherent with conventional AFM [9]. A NSC36 (Mikromasch, Estonia) series was selected as the contacting cantilever, and used most widely in the contact mode. The sampling for measurement with different velocity and cantilever was repeated 12 times in several contact points. Total sampling number of times is 108 (12 times, 3 velocities, and 3 cantilevers). When the tip is approached in the normal direction to the substrate, a smooth surface reveals the adhesion force vertically. However, a surface with highly rough and foreign substance (i.e., dust, organics, and chemicals) has various directional adhesion forces. The morphological effect of the rough and contaminated substrate hindered the analysis of the attraction energy in the normal direction to the substrate. Generally, the mica, as a proof-of-model, provided a <1 nm roughness, and thus was a suitable substrate for measuring the attraction energy in the normal direction to the substrate [10]. The capillary condensation of water might be impacted on the measured adhesion force. To minimize the effect of humidity on measuring the adhesion force, the AFM apparatus was located in the relative humidity (RH) control box, and RH was controlled in the range from 40-50%. Adhesion properties of biomolecules have been reported by researchers, and they identified the distribution of specific functionality via AFM force spectroscopy [11,12]; the adhesive energy was clearly dependent on the contact area. However, in this work we used only one contact area, namely, single tip radius and single

†To whom correspondence should be addressed.
E-mail: korea1@kw.ac.kr

substrate. Therefore, the dependence of adhesion energy on the contact area was minimized in this work.

RESULTS AND DISCUSSION

Local fluid-substrate force interactions, with resolutions in the picoNewtons range, have been reported elsewhere [13]. Different kinds of interactions may be present, including electrostatic, magnetostatic and van der Waals. The van der Waals interactions (F_{vdW}) are omnipresent for a clean, uncharged and nonmagnetic system, and may be the only forces present [14]. This attractive interaction is a function of the separation distance between the tip and the substrate, and does not include the approaching/retracting velocity as variables. However, as revealed in Fig. 1, the attraction force was a function of the velocity (V_z) as well as the tip-sample separation (r). As a function of the velocity, some forces should be considered as repulsive and/or attractive forces to revise the net attraction energy

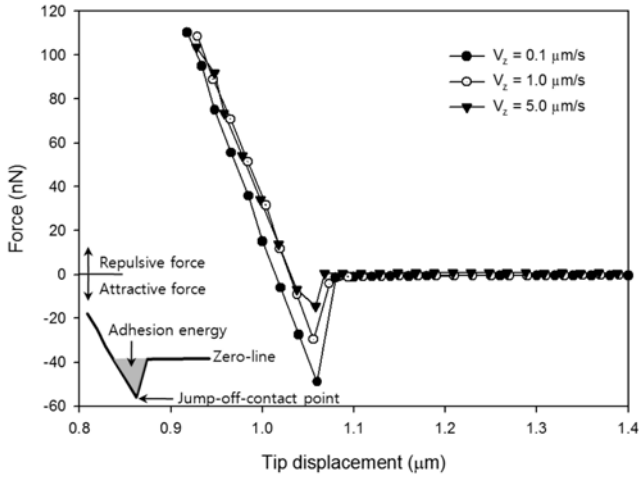

Fig. 1. Experimental F-D curves for mica, as analyzed using NSC36C (L=130 μm and k=0.60 N/m) with different approaching velocities (V_z).

due to the cantilever motion. The net force acting on the approaching/retracting of the tip in the z-direction with V_z includes the drag/squeeze-film (F_{ds}) and normal loading forces (F_{load}). The resulting force acting on the cantilever and tip is as follows:

$$F_{vdW} = \frac{AR^2(1-\sin\gamma)[(R-r)\sin\gamma - R - r]}{6r^2(R+r-R\sin\gamma)^2} - \frac{A\tan\gamma(R+r)\sin\gamma + R\cos(2\gamma)]}{6\cos\gamma(R+r-R\sin\gamma)^2}$$

$$F_{load} = \alpha F_n = \frac{2V_z}{1+(100/\nu)V_z}F_n$$

$$F_{ds} = \mu L V_z\left[\frac{4\pi}{\mathrm{Log}\left(\frac{7.4}{Re}\right)} + \frac{3}{8}\left(\frac{W}{r}\right)^3\right]$$

Where, the parametric notation and detail information for F_{vdW} and F_{ds}/F_{load} can be found in Argento and French's paper [14] and our publication [10], respectively. The values for the parameters used in the equations are summarized in Table 1. F_{vdW} operated at a distance of less than 5-10 nm [15] and, thus, the tip-sample distance in the F-V_z curve was fixed within this range. The acting forces are qualitatively different; F_{vdW} is an intrinsic force and a function of the tip-sample distance (r), while both F_{ds} and F_{load} are extrinsic forces and functions of the approaching velocity (V_z). F_{ds} and F_{load} act as repulsive (positive value) and enforced-attractive (negative value) forces, respectively. Therefore, the net force measured was as follows:

$$F_{net}=F_{tip}+F_{contilever}=(F_{vdW}-F_{load})+F_{ds}=F_{intrinsic}+F_{extrinsic}=F_{vdW}+(F_{ds}-F_{load})$$

F-V_z curves for F_{ds}, F_{vdW}, and F_{total} (=F_{ds}+F_{vdW}) were obtained at a tip-sample distance of 0.01 μm, and analyzed by using NSC36A (Fig. 2). F_{ds} showed an increasing S-shaped curve with respect to V_z, while F_{vdW} had a constant value, because it is not a function of V_z. Therefore, F_{total} mainly followed the increasing shape of F_{ds}, with decreases in the total attractive force with increases in the repulsive force (F_{ds}), namely, more positive forces in the F-D curve. When the tip-sample distance was 10 nm, the effect of F_{ds} was dominant

Table 1. Values of the parameters used in the equations

Parameters	Value or range	Unit	Remark
Hamaker constant, A	1.1×10^{-19}	J	tip (Si_3N_4)-air-mica
Normal force, F_n	39.40, 48.53, 26.74	nN	NSC36A, B, and C
Cantilever length, L	110, 90, 130	ìm	NSC36A, B, and C
Tip radius, R	10	nm	NSC36
Approaching/retracting velocity, V_z	0.1, 1, 5	ìm/s	0 to 50 in calculation
Cantilever width	35	ìm	NSC36
Spring constant, k	0.95, 1.75, 0.60	N/m	NSC36A, B, and C
Resonance frequency	105, 155, 75	kHz	NSC36A, B, and C
Tip-sample distance, r	5 to 10	nm	van der Waals range
Transition parameter, α	0 to 1	-	dimensionless
Cone angle, γ	30	°	NSC36
Viscosity, μ	1.84×10^{-5}	Ns/m^2	air
Kinematic viscosity, ν	0.1546	cSt	air
Density, ρ	0.00119	g/cm^3	air

*Tip height is 20 μm

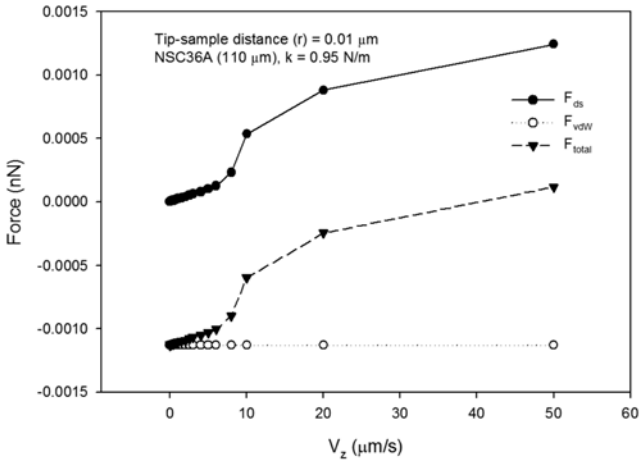

Fig. 2. Calculated F-V_z curves for F_{ds}, F_{vdW} and F_{total} ($=F_{ds}+F_{vdW}$) at a 0.01 μm tip-sample distance, as analyzed using NSC36A.

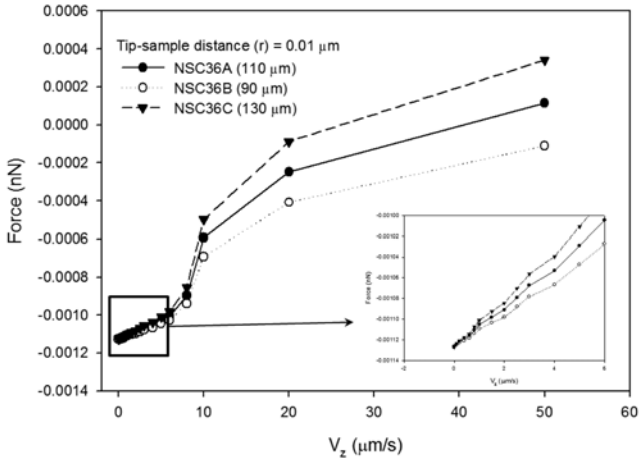

Fig. 3. Calculated F-V_z curves for F_{total} at a 0.01 μm tip-sample distance, as analyzed using NSC36A, NSC36B and NSC36C.

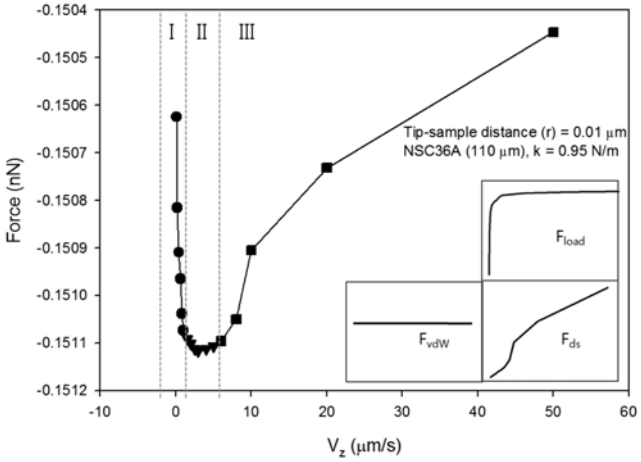

Fig. 4. Calculated F_{net}-V_z curve, with respect to the approaching velocity, at a 0.01 μm tip-sample distance, as analyzed using NSC36A. The inset represents the tendencies of F_{vdW}, F_{load} and F_{ds} in the force-velocity curves.

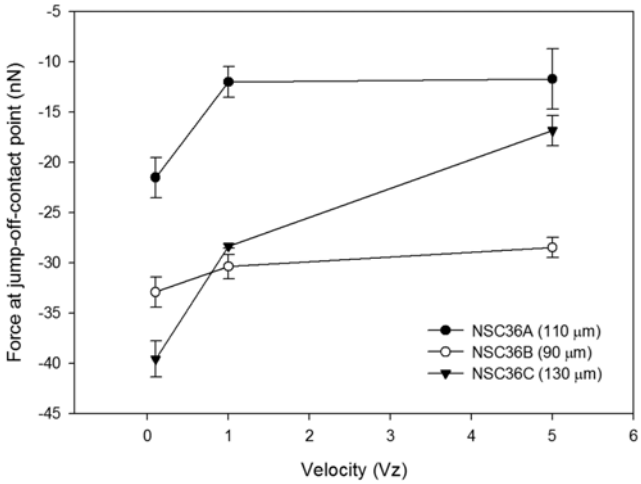

Fig. 5. Experimental F-V_z curves for the NSC36 series cantilever, as obtained at the jump-off-contact point in the force-distance curves.

to that of F_{vdW}, but for an r of 5 nm, the predominance of F_{ds} and F_{vdW} was reversed, as F_{vdW} was superior to any of the other forces in the range <5 nm. This feature could be found with the other cantilevers (NSC36B and NSC36C), as shown in Fig. 3. The cantilever (NSC36C) with a longer length (L) and smaller spring constant (k) was more sensitive to V_z, and easily influenced by the F_{ds} compared to that with NSC36B.

The net force (F_{net}) with a full range of V_z was calculated, and is illustrated in Fig. 4. The F_{net}-V_z curve shows a valley-shaped curve, which could be explained in the summation of the component F_i-V_z curves, such as F_{load}-V_z, F_{vdW}-V_z and F_{ds}-V_z, as shown in the inset figures of Fig. 4. As mentioned before, F_{vdW}-V_z shows a constant value due to the non-function of V_z [14]. F_{load} in the range 0-1 μm/s V_z was dramatically increased, but maintained almost the same value after 1 μm/s V_z [1,10]. Therefore, F_{load} was important within the range 0-1 μm/s V_z. Meanwhile, F_{ds} had an increasing S-shaped curve with respect to V_z and was dominant to the other forces above V_z of 5 μm/s. After the summation of the three F_i-V_z curves, the F_{net}-V_z curve was divided into three regions of forces. In region-I (0-1 μm/s V_z), the net-F_{vdW} was only present at a V_z of 0 μm/s (i.e., $F_{net}=F_{vdW}$), with F_{net} being dramatically decreased, due to the effect of the high increase in F_{load} in the range 0-1 μm/s V_z, which acted as an enforced attractive force (negative force). In region-II (1-5 μm/s V_z), F_{load} was stable above a V_z of 1 μm/s, and thus, F_{net} became stable. In region-III (5-50 μm/s V_z), F_{ds} steadily increased, acting as a repulsive force (positive force) in F_{net}, followed by the increasing shape of the F_{ds}-V_z curve. It should be noted that high-speed analysis of the F-D curve is not recommended due to the effect of the repulsive force (i.e., F_{ds}) between the cantilever and the sample. The net-attraction energy was able to be obtained at approximately zero velocity under conditions of a zero-effect of F_{ds}, while measurement of the F-D curve needs an external loading force (F_{load}) and tip-moving (V_z). Therefore, it is desirable to measure the F-D curve with the velocity range that can minimize the effect of F_{ds}.

Finally, the attractive forces at the jump-off-contact point in the F-D curves were obtained by using NSC36 cantilevers with different V_z, and are displayed in Fig. 5. The jump-off-contact point for

one cantilever at a single V_z was sampled 10 times and then averaged. The force at the jump-off-contact point for NSC36C increased with V_z, which was consistent with the inset figure of Fig. 3. Thus, NSC36C was more sensitive to V_z than NSC36B. This means the short and stiff cantilever, such as NSC36B, was insensitive to increases of V_z, which reduced the F_{ds} effect with respect to V_z. Thus, the attractive force (i.e., adhesion energy) measured with NSC36B was less influenced by the repulsive force (F_{ds}) with respect to V_z. NSC36A has intermediate physical properties to those of NSC36B and NSC36C, and was influenced by F_{ds} up to V_z of 1 μm/s, but the measured force was maintained at a similar value after a V_z of 1 μm/s.

From the literature, the adhesion energy between mica surfaces in air has been reported to be about 70-240 mJ/m^2 [16], or 2.2-7.5×10^{-17} J when considering the contact area of the tip on the mica surface with a normal vector. The contact area of the probe-tip was calculated with respect to the tip-radius, and found to be approximately 3.14×10^{-16} m^2. As represented in the inset figure in Fig. 1, the adhesion energy at the point of Fig. 5 was calculated. NSC36A showed 31, 9.6 and 9.2×10^{-17} J for V_z of 0.1, 1 and 5 μm/s V_z, respectively; whereas, for NSC36B and NSC36C these were 7.2, 6.2 and 5.5×10^{-16} J and 10, 5.3 and 1.9×10^{-16} J, for the same values of V_z, respectively. Some deviations exist between the literature data and those found in the present study, due to differences in the measuring systems used for acquiring the adhesion energy. Namely, the mica-mica (two-parallel plate) interaction was used in literature; whereas, the present study used the mica-tip (cone-plate) system. NSC36B revealed the adhesion energy was less sensitive to F_{ds}-V_z as compared to NSC36A and NSC36B.

CONCLUSIONS

In analyzing the F-D curve, if the approaching/retracting velocity increases, the attraction term in F_{net} reduces, revealing a more positive force due to the increase in the external drag/squeeze-film force. The F_{ds} for a V_z above 5 μm/s gradually increased with respect to V_z, which caused the intrinsic attraction force (F_{vdW}) to diminish. Thus, this feature interfered with the correct measurement of the F_{net}-D curve. It would be reasonable then to assume that for the F-D measured at a V_z less than 1 μm/s, the effect of F_{ds} would diminish with regard to V_z. In addition, based on the sensitive test for length and stiffness of the cantilever, a short, stiff cantilever was found to be the best option to analyze the F-D curve with a high-speed V_z.

ACKNOWLEDGMENT

We are grateful to the Seoul R&BD program for financial support.

REFERENCES

1. S. G. Ansari, M. A. Kar, Y. S. Kim, H. K. Seo, G. S. Kim, R. Wahab, Z. A. Anari, J. M. Seo and H. S. Shin, *Korean J. Chem. Eng*., **25**, 593 (2008).
2. Y. Kim, S. K. Kang, I. Choi, J. Lee and J. Yi, *J. Am. Chem. Soc*., **127**, 9380 (2005).
3. Y. Kim, I. Choi, S. K. Kang, J. Lee and J. Yi, *Appl. Phys. Lett*., **86**, 073113 (2005).
4. B. Cappella and G. Dietler, *Surf. Sci. Rep*., **34**, 1 (1999).
5. V. Heinrich, A. Leung and E. Evans, *J. Chem. Inf. Model*., **45**, 1482 (2005).
6. D. J. Henry, E. Evans and I. Yarovsky, *J. Phys. Chem. B*, **110**, 15963 (2006).
7. G. Yiapanis, D. J. Henry, E. Evans and I. Yarovsky, *J. Phys. Chem. B*, **111**, 6465 (2007).
8. R. W. Carpick, D. F. Ogletree and M. Salmeron, *J. Colloid Interf. Sci*., **211**, 395 (1999).
9. J. Kwon, J. Honh, Y.-S. Kim, D.-Y. Lee, S. Lee and S. Park, *Rev. Sci. Instrum*., **74**, 4378 (2003).
10. Y. Kim and J. Yi, *J. Phys. Chem. B*, **110**, 20526 (2006).
11. E. P. Wojcikiewicz, M. H. Abdulreda, X. Zhang and V. T. Moy, *Biomacromolecules*, **7**, 3188 (2006).
12. H. Kim, H. Arakawa, N. Hatae, Y. Sugimoto, O. Matsumoto, T. Psada, A. Ichikawa and A. Ikai, *Ultramicroscopy*, **106**, 652 (2006).
13. R. E. Jones and D. P. Hart, *Tribol. Int*., **38**, 335 (2005).
14. C. Argento and R. H. French, *J. Appl. Phys*., **80**, 6081 (1996).
15. J. Drelich, Z. Xu and J. Masliyah, *Langmuir*, **22**, 8850 (2006).
16. H. K. Christenson, *J. Phys. Chem*., **97**, 12034 (1993).